Chemistry–A European Journal
Full Paper
doi.org/10.1002/chem.202000962
Chemistry Europe
European Chemical Societies Publishing

Carbonylation |Hot Paper|

Controlling the Depolymerization of Paraformaldehyde with Pd–Phosphine Complexes

Robert Geitner* and Bert M. Weckhuysen*[a]

Abstract: Paraformaldehyde is an easy-to-handle chemical for the in situ generation of formaldehyde and is, therefore, often used in chemistry, structural biology, or medicine. We have investigated the depolymerization process of paraformaldehyde at different temperatures for the application as C1 surrogate in "CO-free" carbonylation reactions using in situ Raman spectroscopy. Rather surprisingly, it was found that small amounts of commonly applied carbonylation catalysts slow down the depolymerization process significantly. By applying ^{1}H, ^{17}O, and ^{31}P NMR spectroscopy coupled with DFT calculations the inhibition process could be assigned to an electron-withdrawing coordination behavior of the Pd complex at the chain end of the paraformaldehyde chain. This inhibition process can be controlled by the utilized phosphine ligand.

Introduction

Carbonylation reactions are one of the most important industrial applications of homogeneous catalysis.[1,2] In a carbonylation reaction a CO molecule is built into an organic substrate which yields a carbonyl compound. Most often the CO molecule is added to an alkene or alkyne whereas the products range from aldehydes over ketons to esters and carboxylic acids depending on the reaction conditions, catalysts and co-substrates.[3]

CO gas is easily available on a large scale, shows the necessary reactivity and is cheap so that it is the CO source of choice for industrial processes like the BASF-oxo process[4,5] and Ruhrchemie/Rhone-Poulenc process.[6,7] Unfortunately CO gas is toxic and it is difficult to handle on a smaller scale or when it cannot be produced on site. To circumvent these drawbacks significant efforts have been undertaken to replace CO gas by so called CO surrogates.[8–12] These CO surrogates are decomposed in situ to yield CO (equivalent) molecules during the carbonylation reaction. The use of CO surrogates lowers the toxicity of carbonylation reactions and thus makes them much easier to handle on a laboratory scale. Important CO surrogates include (*para*)formaldehyde[13–15] and formic acid.[16,17]

Most often these "CO-free" carbonylation reactions are catalyzed by late transition metals like Pd or Rh coordinated by phosphine ligands. The catalyst performs two important tasks: Firstly, it catalyzes the decomposition of the CO surrogate molecule into a CO equivalent species and secondly it catalyzes the actual carbonylation reaction using the prior generated CO equivalent. Thus, it is of utmost importance to fully understand the role of the catalyst to improve the rate, yield and selectivity of „CO-free" carbonylation reactions. The mechanism of carbonylation reactions is well understood when CO gas is used.[18] In contrast to this there are very few reports that investigate the reaction mechanism when a CO surrogate is used instead of CO gas[19–21] and unfortunately even less is known about the depolymerization of paraformaldehyde[22,23] in solution and the influence of homogeneous catalysts on the depolymerization process.

In this context, it is interesting to investigate the interaction between homogeneous Pd catalysts and the CO surrogate paraformaldehyde to fully understand all steps of "CO-free" carbonylation reactions. Naturally the depolymerization of paraformaldehyde is the starting point of these reactions. This study focusses on the depolymerization of paraformaldehyde and the influence of the commonly used carbonylation catalysts $[Pd(d^tbpx)]^{2+}$ (d^tbpx = 1,2-Bis(di-tert-butylphosphinomethyl) benzene) and $[Pd(dppp)]^{2+}$ (dppp = 1,3-Bis(diphenylphosphino) propane) on this depolymerization reaction. By using a combination of in situ Raman spectroscopy, ^{1}H, ^{31}P, and ^{17}O NMR spectroscopy as well as density functional theory (DFT) calculations we show that $[Pd(d^tbpx)]^{2+}$ based complexes raise the activation energy for the paraformaldehyde depolymerization by more than two times and that this surprising result can be explained by the complexation behavior of $[Pd(d^tbpx)]^{2+}$ fragments towards the chain end of the paraformaldehyde molecule. We show that this coordination lowers the electron density at important oxygen atoms which in turn inhibits the depolymerization reaction. Furthermore, we

[a] Dr. R. Geitner, Prof. Dr. B. M. Weckhuysen
Inorganic Chemistry and Catalysis Group
Debye Institute for Nanomaterials Science
Utrecht University, Universiteitsweg 99, 3584 CG Utrecht (The Netherlands)
E-mail: r.geitner@uu.nl
b.m.weckhuysen@uu.nl

Supporting information and the ORCID identification number(s) for the author(s) of this article can be found under: https://doi.org/10.1002/chem.202000962.

were able to control this inhibitory process by switching from $[Pd(d^tbpx)]^{2+}$ to $[Pd(dppp)]^{2+}$.

Results and Discussion

To investigate in more detail the kinetics of the paraformaldehyde depolymerization in situ Raman spectroscopy was applied. Raman spectroscopy is an ideal characterization method for this task as it can measure the concentration of $H_2C(OMe)_2$, which is the product of the paraformaldehyde depolymerization in methanol (see Scheme 1) contactless inside the pressurized reactor. To monitor the $H_2C(OMe)_2$ concentration the ν_S(O-C-O) vibration at 913 cm^{-1}[24] was utilized, while the ν(C-O) vibration of methanol[25] was used as an internal reference. Figure 1a shows some representative Raman spectra, which have been background corrected and normalized, after being collected during the depolymerization of paraformaldehyde in MeOH at 90 °C. To evaluate the influence of the potential carbonylation catalyst $[Pd(d^tbpx)]^{2+}$ and the influence of temperature the Raman measurements were conducted at different temperatures with and without Pd-phosphine complexes present.

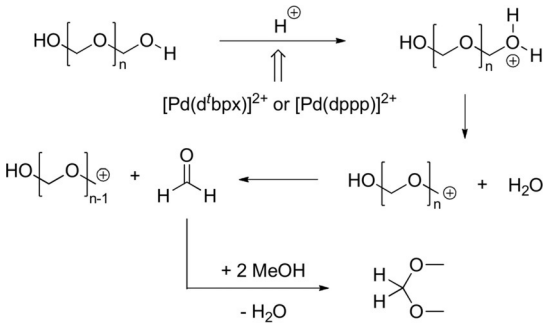

Scheme 1. Acid induced depolymerization of paraformaldehyde and acetal formation of formaldehyde in methanol.

To extract kinetic information on the depolymerization of paraformaldehyde only the data points where the final measurement temperature has been reached (see Figure S4) were used for a first-order kinetic fit. For example, selected data points and their exponential first-order kinetic fit can be seen in Figure 1b. The following equation was used as the kinetic model [Eq (1)]:

$$P = P_0 \cdot e^{-k \cdot t} + P_f \quad (1)$$

where t is the time, k the temperature dependent kinetic constant, P the peak area of the ν_S(O-C-O) vibration, P_0 the starting peak area and P_f the final peak area. A first-order kinetic model was used because it gave the best fit to the data compared to a zeroth- order model (see SI for extended discussion) and is in line with polymerization experiments of formaldehyde.[23] The results of the fitting procedure are summarized in Table 1. Furthermore, the extracted temperature-dependent kinetic constants were used in an Arrhenius plot to evaluated the activation energy E_A of the paraformaldehyde depolymerization. The following Arrhenius equation was used [Eq. (2)]:

$$\ln(k) = \ln(A) - \frac{E_A}{R}\left(\frac{1}{T}\right) \quad (2)$$

in which A is the pre-exponential factor, T the absolute temperature and R the gas constant.

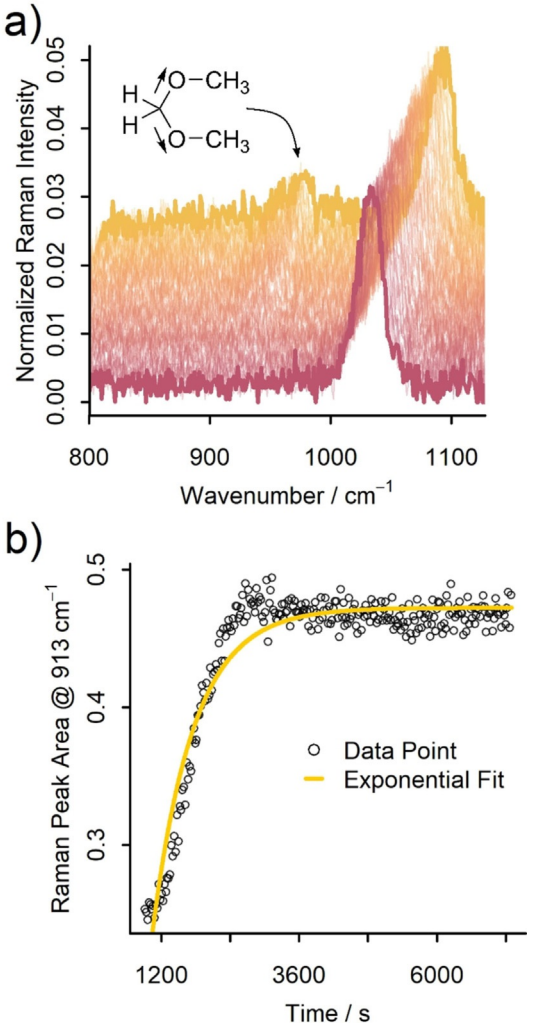

Figure 1. a) Showcase background corrected and normalized in situ Raman spectra collected during the depolymerization of paraformaldehyde in MeOH at 90 °C with $[Pd(d^tbpx)]^{2+}$ from 0 to 7200 s. b) Raman peak area of the ν_S(O-C-O) vibration plotted against reaction time. Each point is the average from 20 individual Raman spectra. The peak area corresponds to the formation of $H_2C(OMe)_2$ and thus serves as an indicator for the depolymerization of paraformaldehyde. These data points were recorded under thermostatic conditions. To analyze the kinetic parameters of the depolymerization the data points were fitted with a first-order exponential function. See Table 1 for rate constants.

As can be seen from Table 1 the depolymerization process of paraformaldehyde is significantly slowed down when even catalytic amounts (0.15 mol%) of the common carbonylation catalyst $[Pd(d^tbpx)(MeOH)_2]^{2+}$ are present in solution. $[Pd(d^tbpx)]^{2+}$ fragments formed from $[Pd(d^tbpx)(MeOH)_2]^{2+}$ act as inhibitors in this reaction. This finding is also solidified by the calculated activation energies: When $[Pd(d^tbpx)]^{2+}$ frag-

Table 1. Kinetic significant digits of paraformaldehyde depolymerization as derived from in situ Raman spectroscopy measurements.

	w/o cat	$[Pd(d^tbpx)]^{2+}$	d^tbpx	$[Pd(dppp)]^{2+}$	dppp	NaOAc
$k(60\,^\circ C)\times10^{-4}$ [s^{-1}]	11	–	10	–	3	8
$k(70\,^\circ C)\times10^{-4}$ [s^{-1}]	22	1	8	3	14	18
$k(80\,^\circ C)\times10^{-4}$ [s^{-1}]	31	1	20	8	14	25
$k(90\,^\circ C)\times10^{-4}$ [s^{-1}]	54	7	26	16	25	–
$k(100\,^\circ C\times10^{-4}$ [s^{-1}]	79	20	40	24	66	–
E_A [kJ mol^{-1}]	50	141	39	71	67	57
$\sigma(E_A)$ [kJ mol^{-1}]	4	16	15	7	22	14

ments are present in solution the activation energy is nearly three times larger (141 vs. 50 kJ mol^{-1}) for the paraformaldehyde depolymerization compared to when the inhibitor is not part of the reaction.

This strong influence of $[Pd(d^tbpx)]^{2+}$ raised two questions: (1) Why does even a small amount of the Pd complex have such a drastic influence on the depolymerization reaction and (2) how does the Pd complex interact with the paraformaldehyde molecule? To study the coordination behavior of $[Pd(d^tbpx)]^{2+}$ and paraformaldehyde a combined DFT and NMR approach was used. To model paraformaldehyde in quantum chemical calculations the oligomer $MeO(CH_2O)_4H$ was used. $MeO(CH_2O)_4H$ is small enough to be analyzed by DFT calculations in a reasonable time frame while simultaneously featuring all important molecular structures of paraformaldehyde.

First, the DFT calculations were focused on the coordination behavior of the $[Pd(d^tbpx)]^{2+}$ fragment towards $MeO(CH_2O)_4H$. The DFT calculations revealed that $MeO(CH_2O)_4H$ favors a κ^2-O-OH coordination mode at the $[Pd(d^tbpx)]^{2+}$ fragment (see Figure 2). This indicates that paraformaldehyde chains probably coordinate with their chain end to the $[Pd(d^tbpx)]^{2+}$ fragment. This affinity for the paraformaldehyde chain end could explain why a small amount of $[Pd(d^tbpx)]^{2+}$ based complexes has a large influence on the depolymerization. Each paraformaldehyde chain features only two chain ends which in turn lowers the effective concentration of reactive groups for the depolymerization process. Taken together with the low solubility of paraformaldehyde in MeOH even a low concentration of $[Pd(d^tbpx)]^{2+}$ fragments can be enough to selectively coordinate to all available paraformaldehyde chain ends. As the depolymerization reaction starts at the chain end (see Scheme 1) any modification to the molecular and electronic structure of the chain end will have a drastic influence on the depolymerization of paraformaldehyde.

To strengthen the insights gained from DFT calculations a series of NMR spectra were recorded (see Figures S5 and S16) and combined with additional DFT calculations. The goal of the NMR measurements was to evaluate the experimental binding behavior of $[Pd(d^tbpx)]^{2+}$ fragments towards different oxygen donors. To the best of our knowledge there is no synthesis available to selectively generate formaldehyde oligomers, like $MeO(CH_2O)_4H$. To model the potentially multidentate coordination behavior of paraformaldehyde featuring alcohol and ether groups THF, diglyme, 2-methoxy ethanol (2-MeOEtOH) and MeOH were used. $Pd(OAc)_2$ and d^tbpx were dissolved in a non-coordinating solvent ($DCCl_3$) while the oxygen donors were added stepwise to the mixture. The results are summarized in Scheme 2.

Unfortunately, it was not possible to unambiguously identify the structure of the Pd^{II}-d^tbpx complex in pure $DCCl_3$. The complex shows two ^{31}P signals at 21 and 108 ppm indicating an asymmetric species. We suspect an acetate bridged, multi-

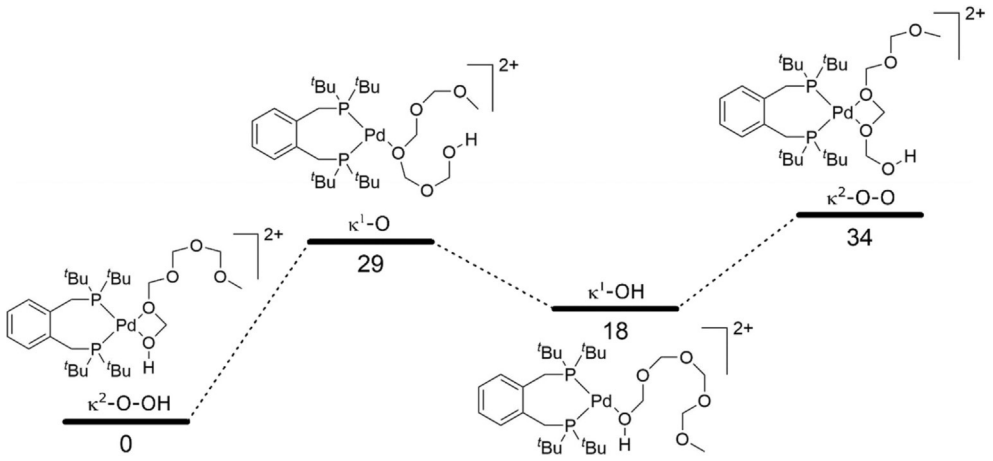

Figure 2. Relative Density Functional Theory (DFT) calculated free energies (in kJ mol^{-1}) for $[Pd(d^tbpx)(MeO(CH_2O)_4H)]^{2+}$. The paraformaldehyde model $MeO(CH_2O)_4H$ can coordinate in four different ways to the $[Pd(d^tbpx)]^{2+}$ fragment: κ^2-O-OH, κ^1-O, κ^1-OH and κ^2-O-O.

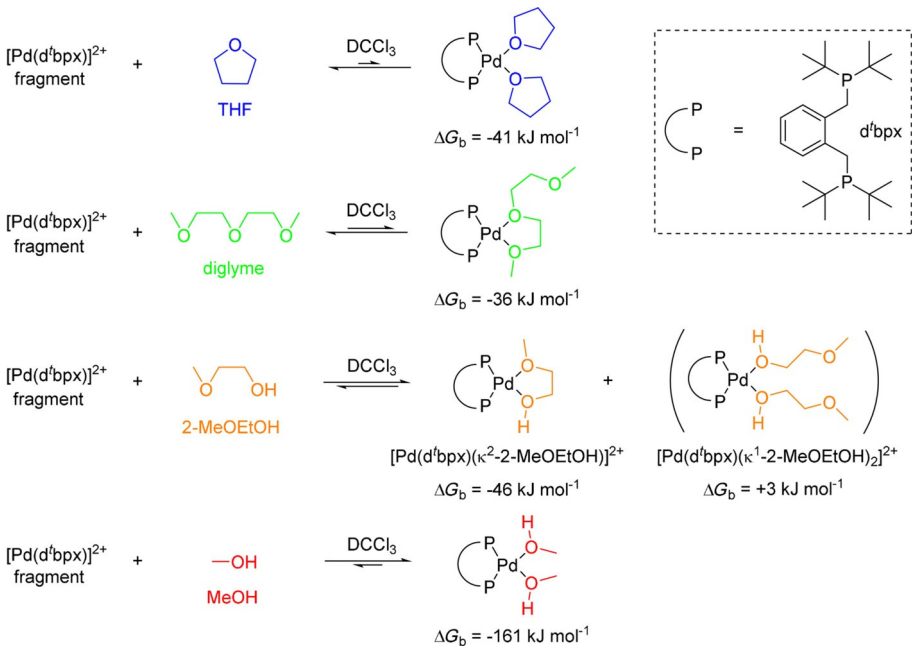

Scheme 2. Results of co-solvent dependent NMR spectra and DFT calculated bindings energies to the $[Pd(d^tbpx)]^{2+}$ fragment.

core Pd^{II}-d^{t}bpx complex. The NMR experiments revealed that the binding affinity of the oxygen donors increases from THF over diglyme and 2-MeOEtOH to MeOH. All resulting $[Pd(d^tbpx)(solv)_{1-2}]^{2+}$ species are characterized by a single ^{31}P signal at around 58 ppm.[26] This indicates that the $[Pd(d^tbpx)(solv)_{1-2}]^{2+}$ complexes are symmetric on the NMR time scale that thus the exchange rates of the solvent molecules at the $[Pd(d^tbpx)]^{2+}$ fragment must be fast. An additional low temperature experiment at −65 °C for 2-MeOEtOH (see Figures S17-S18) showed a significant line broadening for the ^{31}P signal at 59.6 ppm which indicates that the two phosphorus atoms in d^{t}bpx become inequivalent at lower temperatures. Therefore, it can be concluded that only one and not two molecules of 2-MeOEtOH coordinates to the $[Pd(d^tbpx)]^{2+}$ fragment. This is backed up by DFT calculations showing that the binding energy ΔG_b for $[Pd(d^tbpx)(\kappa^2\text{-}2\text{-MeOEtOH})]^{2+}$ is larger than for $[Pd(d^tbpx)(\kappa^1\text{-}2\text{-MeOEtOH})_2]^{2+}$ (−46 vs. +3 kJ mol^{-1}). Overall the NMR measurements showed that alcoholic oxygen atoms have a stronger affinity towards $[Pd(d^tbpx)]^{2+}$ fragments than etheric oxygens and that a κ^2-O-OH coordination mode is possible at the Pd complex. These findings support the hypothesis of the chain end κ^2-O-OH coordination of paraformaldehyde to the $[Pd(d^tbpx)]^{2+}$ fragment.

As pointed out earlier the influence of the $[Pd(d^tbpx)]^{2+}$ fragment on the structure of the paraformaldehyde chain end is detrimental to control its influence on the paraformaldehyde depolymerization reaction. As can be seen from Scheme 1 the paraformaldehyde depolymerization starts with a protonation of the alcohol group at the chain end. We propose that the change in electron density at the relevant oxygen atoms due to the coordination of the $[Pd(d^tbpx)]^{2+}$ fragment significantly inhibits the protonation step and thus the depolymerization process.

To investigate the change in electron density, again a combination of DFT calculations and NMR measurements was used. To find out about the electron density at the coordinating oxygen atoms (illustrated in Figure 3) ^{17}O NMR spectroscopy was combined with Voronoi density deformation (VDD) values from DFT calculations. VDD is—just like Mullikan charges—a concept to describe formal charges at individual atoms.[27,28] Smaller values indicate a high electron density at the respective atom while a large value indicates an atom with low elec-

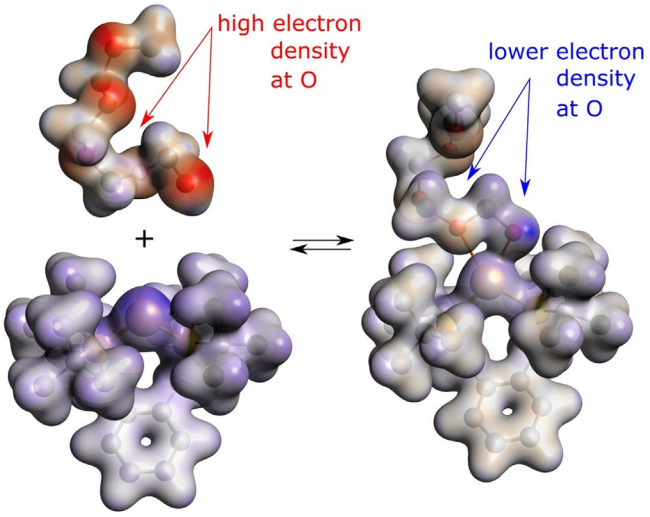

Figure 3. DFT calculated geometries and electron densities for $MeO(CH_2O)_4H$, the $[Pd(d^tbpx)]^{2+}$ fragment and $[Pd(d^tbpx)(MeO(CH_2O)_4H)]^{2+}$ (κ^2-O-OH coordination mode, hydrogen atoms omitted for clarity). Red color means high electron density while blue color indicates a low electron density. The reduced electron density at the coordinating oxygen atoms in $[Pd(d^tbpx)(MeO(CH_2O)_4H)]^{2+}$ is clearly visible.

tron density. To probe the theoretical calculated formal charges NMR spectroscopy was used. The chemical shift of an atom depends on the electron density around the nucleus and thus the chemical shift can be used as an indicator for the electron density at a specific atom. Consequently, ^{17}O NMR spectroscopy was used to investigate the electron density at the coordinating oxygen atoms.

Unfortunately, ^{17}O has a low natural abundance and low NMR sensitivity so that reasonable signals can only be obtained for pure substances or ^{17}O enriched samples. As an example to link theoretical VDD values and ^{17}O NMR shifts $[Pd(d^tbpx)(MeOH)_2]^{2+}$ was measured in ^{17}O enriched methanol.

As can be seen from Table 2 the oxygen atom in MeOH has a VDD value of −0.251 and a ^{17}O chemical shift of −33.7 ppm (see Figure 4). In contrast to this MeOH coordinated to the $[Pd(d^tbpx)]^{2+}$ fragment has a VDD value of −0.210 and a ^{17}O shift of 27.9 ppm (see inset in Figure 4). It can be seen that MeOH coordinates via the oxygen atom to the palladium ion and that the electron density at the oxygen is reduced by this coordination behavior. Therefore, the VDD value as well as the chemical shift indicate that the coordinated oxygen atom behaves more like an etheric oxygen atom (^{17}O shift Et_2O: 16.6 ppm) then like an alcoholic oxygen atom.

As the other oxygen donors used in this study are not available as ^{17}O enriched samples the calculated VDD values will be used to gain insight into the oxygen electron density for the other co-ligands (see Table S1). As can be expected from the coordination experiment in methanol the electron density at all coordinating oxygen atoms decreases. The change in electron density is more pronounced for coordinating alcoholic oxygen atoms (+0.046) than for coordinating etheric ones (+0.013). The $[Pd(d^tbpx)(MeO(CH_2O)_4H)]^{2+}$ complex is no different in this case.

As initially proposed the electron density at the coordinating oxygen atoms is reduced and thus most likely the protonation at the paraformaldehyde chain end is inhibited.

With the results from DFT calculations and NMR spectroscopy in mind it can be concluded that the end of the paraformaldehyde polymer chain coordinates with two oxygen atoms to the $[Pd(d^tbpx)]^{2+}$ fragment and that this coordination behavior lowers the electron density at the oxygen atoms significantly. The reduced electron density makes an electrophilic attack of a proton, which is the first step in the depolymerization of paraformaldehyde, less likely/more energy intense. This result is in line with the initially observed inhibitory influence of $[Pd(d^tbpx)]^{2+}$ fragments on the depolymerization of paraformaldehyde which induced a very high activation energy (141 kJ mol^{-1}) for the depolymerization.

Considering the electronic and structural influence of the $[Pd(d^tbpx)]^{2+}$ fragment on paraformaldehyde it should be possible to control the inhibitory properties of the Pd complex by changing the utilized diphosphine. For a proof-of-concept study dppp was chosen. It is not as rigid as d^tbpx and the electronic structure at the coordinating phosphorus atoms is altered by exchanging the *tert*-butyl groups for phenyl groups. In case of a coordination the phenyl groups should stabilize the system via their M-effect.

As can be seen from Table 1 the activation energy drops significantly when $[Pd(dppp)]^{2+}$ based complexes are used instead of $[Pd(d^tbpx)]^{2+}$ based ones (51 vs. 141 kJ mol^{-1}). Using DFT calculations (see Table S1) it can also be shown that the electron-withdrawing effect of the $[Pd(dppp)]^{2+}$ fragment at the coordinating OH group in $[Pd(dppp)(MeO(CH_2O)_4H)]^{2+}$ (κ^2-O-OH) is slightly weaker than the electron-withdrawing effect of the $[Pd(d^tbpx)]^{2+}$ fragment. This experiment nicely proves that the inhibitory properties of palladium complexes can be tuned by altering the diphosphine ligand structure. This enables a tool for the controlled release of formaldehyde especially during „CO-free" carbonylation reactions.

Table 2. ^{17}O NMR shifts and DFT-calculated VDD of oxygen containing species.

Compound	^{17}O shift(s) [ppm]	VDD
MeOH	−33.7	−0.251
EtOH	8.3	−0.249
Et_2O	16.6	−0.185
THF	18.8	−0.210
diglyme–C_2H_4-O-C_2H_4	−1.3	−0.192
–O-Me	−21.8	−0.187
2-methoxy ethanol–O-H	−3.3	−0.254
–O-Me	−21.9	−0.200
$[Pd(d^tbpx)(MeOH)_2]^{2+}$	27.9	−0.210

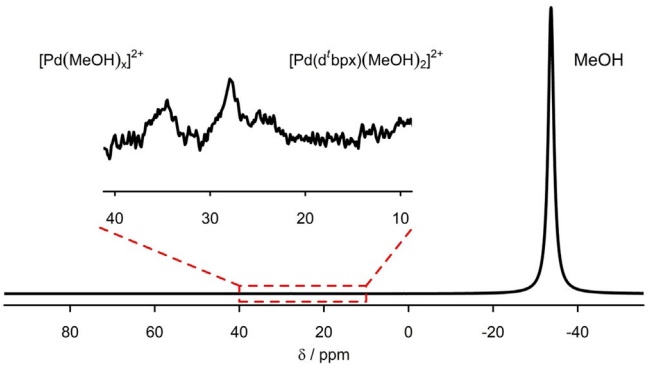

Figure 4. ^{17}O NMR of $[Pd(d^tbpx)(MeOH)_2]^{2+}$ in ^{17}O enriched methanol (20 mol%). The low field shift from −33.7 to 27.9 ppm indicates that the electron density at the coordinating oxygen atoms is reduced by the $[Pd(d^tbpx)]^{2+}$ fragment. The signal at 34.5 ppm can be assigned to solvated Pd^{2+} ions by adding additional $Pd(OAc)_2$.

Conclusions

The present study nicely demonstrates how even small amounts of a metal complex can drastically alter the reactivity of paraformaldehyde by changing the electron density at its reactive sites. We demonstrated an inhibitory influence of Pd complexes on the depolymerization of paraformaldehyde and showed how the properties of the homogeneous catalyst can be studied and consecutively tuned to meet the need for control. We believe that the discovered inhibitory effect and how it can be controlled is very important to fully understand the

depolymerization of paraformaldehyde especially in the context of „CO-free" carbonylation reactions.

Experimental Section

All experimental details (Raman spectra, NMR spectra, NMR assignments, DFT calculated structures and DFT calculated IR spectra) are described in the Supporting Information.

Acknowledgements

R.G. gratefully acknowledges a Research Scholarship from the German Science Foundation (DFG) under the grant number GE3112/2-1. The authors would like to thank Johan Jastrzebski for assistance during the advanced NMR measurements and the Organic Chemistry and Catalysis (OCC) group at Utrecht University for providing NMR measurement time. Furthermore, the authors would like to thank Dr. Rosa Bulo for the computational time at the Obi1 computer cluster at Utrecht University.

Conflict of interest

The authors declare no conflict of interest.

Keywords: carbonylation · density functional calculations · nuclear magnetic resonance · Pd · Raman spectroscopy

[1] W. Bertleff, M. Roeper, X. Sava, *Ullmann's Encyclopedia of Industrial Chemistry* **2000**, *582*, 94 – 113.
[2] M. Beller, *Catalytic Carbonylation Reactions*, Springer, London, **2006**.
[3] M. Beller, B. A. Steinhoff, J. R. Zoeller, D. J. Cole-Hamilton, E. Drent, X.-F. Wu, H. Neumann, S. Ito, K. Nozaki in *Applied Homogeneous Catalysis with Organometallic Compounds* (Eds.: B. Cornils, W. A. Herrmann, M. Beller, R. Paciello), Wiley-VCH, Weinheim, **2017**, pp. 91 – 190.
[4] H.-J. Blankertz, A. V. Grenacher, F. Sauer, H. Schwahn, W. Schönmann, M. Röper, Hydroformylation process (US6331656 B1).
[5] G. Dümbgen, D. Neubauer, *Chem. Ing. Tech.* **1969**, *41*, 974 – 980.
[6] W. A. Herrmann, C. W. Kohlpaintner, *Angew. Chem.* **1993**, *105*, 1588 – 1609.
[7] E. Wiebus, B. Cornils, *Chem. Ing. Tech.* **1994**, *66*, 916 – 923.
[8] T. Morimoto, K. Kakiuchi, *Angew. Chem. Int. Ed.* **2004**, *43*, 5580 – 5588; *Angew. Chem.* **2004**, *116*, 5698 – 5706.
[9] P. Hermange, A. T. Lindhardt, R. H. Taaning, K. Bjerglund, D. Lupp, T. Skrydstrup, *J. Am. Chem. Soc.* **2011**, *133*, 6061 – 6071.
[10] L. Wu, Q. Liu, R. Jackstell, M. Beller, *Angew. Chem. Int. Ed.* **2014**, *53*, 6310 – 6320; *Angew. Chem.* **2014**, *126*, 6426 – 6436.
[11] P. Gautam, B. M. Bhanage, *Catal. Sci. Technol.* **2015**, *5*, 4663 – 4702.
[12] J. Cao, Z.-J. Zheng, Z. Xu, L.-W. Xu, *Coord. Chem. Rev.* **2017**, *336*, 43 – 53.
[13] T. Okano, T. Kobayashi, H. Konishi, J. Kiji, *Tetrahedron Lett.* **1982**, *23*, 4967 – 4968.
[14] W. Li, X.-F. Wu, *Adv. Synth. Catal.* **2015**, *357*, 3393 – 3418.
[15] K. Fuji, T. Morimoto, K. Tsutsumi, K. Kakiuchi, *Angew. Chem. Int. Ed.* **2003**, *42*, 2409 – 2411; *Angew. Chem.* **2003**, *115*, 2511 – 2513.
[16] R. Sang, P. Kucmierczyk, K. Dong, R. Franke, H. Neumann, R. Jackstell, M. Beller, *J. Am. Chem. Soc.* **2018**, *140*, 5217 – 5223.
[17] L. Wang, H. Neumann, M. Beller, *Angew. Chem. Int. Ed.* **2018**, *57*, 6910 – 6914; *Angew. Chem.* **2018**, *130*, 7026 – 7030.
[18] K. Dong, X. Fang, S. Gülak, R. Franke, A. Spannenberg, H. Neumann, R. Jackstell, M. Beller, *Nat. Commun.* **2017**, *8*, 14117.
[19] M. Rosales, H. Pérez, F. Arrieta, R. Izquierdo, C. Moratinos, P. J. Baricelli, *J. Mol. Catal. A: Chem.* **2016**, *421*, 122 – 130.
[20] K. Dong, R. Sang, Z. Wei, J. Liu, R. Dühren, A. Spannenberg, H. Jiao, H. Neumann, R. Jackstell, R. Franke, M. Beller, *Chem. Sci.* **2018**, *9*, 2510 – 2516.
[21] Q. Liu, K. Yuan, P.-B. Arockiam, R. Franke, H. Doucet, R. Jackstell, M. Beller, *Angew. Chem. Int. Ed.* **2015**, *54*, 4493 – 4497; *Angew. Chem.* **2015**, *127*, 4575 – 4580.
[22] E. J. Grajales, E. A. Alarcón, A. L. Villa, *Thermochim. Acta* **2015**, *609*, 49 – 60.
[23] O. Vogl, *J. Macromol. Sci.* **1975**, *12*, 109 – 164.
[24] N. Lebrun, P. Dhamelincourt, C. Focsa, B. Chazallon, J. L. Destombes, D. Prevost, *J. Raman Spectrosc.* **2003**, *34*, 459 – 464.
[25] G. Socrates, *Infrared and Raman Characteristic Group Frequencies: Tables and Charts*, Wiley, West Sussex, **2007**.
[26] W. Clegg, G. R. Eastham, M. R. J. Elsegood, B. T. Heaton, J. A. Iggo, R. P. Tooze, R. Whyman, S. Zacchini, *Organometallics* **2002**, *21*, 1832 – 1840.
[27] C. Fonseca Guerra, J.-W. Handgraaf, E. J. Baerends, F. M. Bickelhaupt, *J. Comput. Chem.* **2004**, *25*, 189 – 210.
[28] C. Fonseca Guerra, J. G. Snijders, G. te Velde, E. J. Baerends, *Theor. Chem. Acc.* **1998**, *99*, 391 – 403.

Manuscript received: February 23, 2020
Revised manuscript received: February 29, 2020
Accepted manuscript online: March 2, 2020
Version of record online: April 1, 2020